Cancer Cell
Article

Constitutive Canonical NF-κB Activation Cooperates with Disruption of *BLIMP1* in the Pathogenesis of Activated B Cell-like Diffuse Large Cell Lymphoma

Dinis Pedro Calado,[1,6] Baochun Zhang,[1,6] Lakshmi Srinivasan,[1] Yoshiteru Sasaki,[1,4] Jane Seagal,[1] Christine Unitt,[2] Scott Rodig,[2] Jeffery Kutok,[2] Alexander Tarakhovsky,[3] Marc Schmidt-Supprian,[1,5] and Klaus Rajewsky[1,*]
[1]Program of Cellular and Molecular Medicine, Children's Hospital, and Immune Disease Institute, Harvard Medical School, Boston, MA 02115, USA
[2]Department of Pathology, Brigham and Women's Hospital, Boston, MA 02115, USA
[3]Laboratory of Lymphocyte Signaling, The Rockefeller University, New York, NY 10065, USA
[4]Riken Center for Developmental Biology, Kobe, Hyogo 650-0047, Japan
[5]Max Planck Institute of Biochemistry, Am Klopferspitz 18, D-82152 Martinsried, Germany
[6]These authors contributed equally to this work
*Correspondence: rajewsky@idi.harvard.edu
DOI 10.1016/j.ccr.2010.11.024

SUMMARY

Diffuse large B cell lymphoma (DLBCL) comprises disease entities with distinct genetic profiles, including germinal center B cell (GCB)-like and activated B cell (ABC)-like DLBCLs. Major differences between these two subtypes include genetic aberrations leading to constitutive NF-κB activation and interference with terminal B cell differentiation through *BLIMP1* inactivation, observed in ABC- but not GCB-DLBCL. Using conditional gain-of-function and/or loss-of-function mutagenesis in the mouse, we show that constitutive activation of the canonical NF-κB pathway cooperates with disruption of *BLIMP1* in the development of a lymphoma that resembles human ABC-DLBCL. Our work suggests that both NF-κB signaling, as an oncogenic event, and BLIMP1, as a tumor suppressor, play causal roles in the pathogenesis of ABC-DLBCL.

INTRODUCTION

Diffuse large B cell lymphoma (DLBCL) is the most frequent lymphoid malignancy, representing 30%–40% of all non-Hodgkin lymphomas (Lenz and Staudt, 2010; WHO, 2008). DLBCL comprises disease entities with distinct gene expression signatures and response to therapy. Indeed, studies using gene expression profiling have classified various subtypes of DLBCL according to their putative cell of origin (COO) or consensus clusters (Alizadeh et al., 2000; Monti et al., 2005). In the COO classification, two main subgroups of DLBCL emerged. One is the germinal center B cell (GCB)-like DLBCL, which has a gene expression profile that closely resembles that of normal germinal center (GC) B cells. The other is activated B cell (ABC)-like DLBCL, with a gene expression profile resembling that of in vitro ABCs (Alizadeh et al., 2000).

DLBCLs carry somatically mutated rearranged immunoglobulin (Ig) V region genes (Lenz and Staudt, 2010; Lossos et al., 2000). Although somatic hypermutation (SHM) of Ig genes may not be entirely GC specific, the GCB-DLBCL gene expression profile in conjunction with often ongoing SHM strongly suggests that this lymphoma is indeed derived from a GC B cell. In the case of ABC-DLBCL, the COO is less clearly defined and may be either a late GC B cell, an activated post-GC, or even a GC unrelated B cell (Lenz and Staudt, 2010).

A major difference between GCB-DLBCL and ABC-DLBCL is constitutive NF-κB activity in the latter (Alizadeh et al., 2000; Staudt, 2010). NF-κB signaling plays a crucial role in B cell physiology and can make B cells independent of survival factors, such as BAFF (Sasaki et al., 2006). Similarly, ABC- but not GCB-DLBCL relies on constitutive activity of the canonical

Significance

ABC-DLBCL is the most aggressive DLBCL and has a poor clinical prognosis. Constitutive NF-κB activity interferes with the apoptotic effect of chemotherapy and may account for the poor response to treatment of patients with ABC-DLBCL. Our studies in the mouse improve the understanding of human ABC-DLBCL pathogenesis by the demonstration that two recurrent events in this disease, constitutive NF-κB activity and abrogation of terminal B cell differentiation through *BLIMP1* disruption, cooperate in lymphomagenesis. Because of the similarity of the lymphomas arising in the compound mutants with human ABC-DLBCL, these mice may serve as a preclinical model for this disease and be used to identify additional oncogenic events and new therapeutic targets.

NF-κB pathway for survival (Davis et al., 2001; Staudt, 2010). Recently, mutations leading to constitutive canonical NF-κB activation in ABC-DLBCL have been described (Compagno et al., 2009; Davis et al., 2010; Kato et al., 2009; Lenz et al., 2008a). Another characteristic of ABC-DLBCL is genetic alterations that interfere with terminal B cell differentiation. Thus, ~25% of ABC-DLBCLs show inactivating mutations of BLIMP1 (Pasqualucci et al., 2006; Tam et al., 2006), a key regulator of plasma cell differentiation (Martins and Calame, 2008), suggesting that BLIMP1 may function as a tumor suppressor in the pathogenesis of ABC-DLBCL. Additional recurrent mutations in ABC-DLBCL that block plasma cell differentiation include genetic aberrations resulting in deregulated expression of *SPIB* (~26%) or *BCL6* (~24%) (Iqbal et al., 2007; Lenz and Staudt, 2010; Lenz et al., 2008b).

In an attempt to assess the roles of NF-κB activation and *BLIMP1* disruption in the pathogenesis of ABC-DLBCL, we used a genetic system in the mouse that allows conditional gain-of-function and/or loss-of-function mutagenesis in GC B cells.

RESULTS

Experimental Design

For targeted mutagenesis in GC B cells, we used the *Cγ1-cre* transgene, expressed in B cells at early stages of the GC reaction (Casola et al., 2006). To induce activation of the NF-κB canonical pathway, we combined this transgene with a *ROSA26* allele, termed *IKK2ca*^{stopFL}, that harbors a cDNA encoding a constitutively active IKK2 protein, which mediates canonical but not alternative NF-κB activation, preceded by a *loxP* flanked STOP cassette (Sasaki et al., 2006). We complemented this system by introducing a conditional *BLIMP1* allele (*Blimp1*^{F}; Ohinata et al. [2005]), alone or in combination with *IKK2ca*^{stopFL}. Activation of the *IKK2ca*^{stopFL} allele by Cre-mediated recombination is marked by expression of GFP under the control of an internal ribosomal entry site downstream of the inserted IKK2ca cDNA. To report Cre-mediated recombination in cells carrying the *Blimp1*^{F} allele, we combined it with a *ROSA26* reporter allele harboring an YFP gene preceded by a *loxP* flanked STOP cassette (*eYFP*^{stopFL}; Srinivas et al. [2001]). Mice carrying the *Cγ1-cre* transgene in combination with *eYFP*^{stopFL} served as controls.

Impact of NF-κB Activation and *BLIMP1* Deletion on the GC Reaction and B Cell Proliferation and Survival In Vitro

To determine the impact of enforced NF-κB activation and/or disruption of *BLIMP1* on the GC reaction, we examined splenic GC B cells in control and experimental mice upon immunization with sheep red blood cells (SRBCs). Mice with *BLIMP1* deletion alone showed increased numbers of GC B cells at day 10 after primary immunization (Figures 1A and 1C), a trend that persisted to day 21 and upon secondary immunization (Figures 1B and 1C). In contrast, mice with enforced expression of *IKK2ca* alone showed some reduction in the GC B cell fraction at day 10 after primary (Figures 1A and 1C) and secondary immunization (Figure 1C), to which the increased *BLIMP1* levels in these cells may contribute (Figure 1D) (Martins and Calame, 2008). Indeed, concomitant *BLIMP1* disruption overrode this effect and, like deletion of *BLIMP1* alone, led to increased numbers of GC B cells (Figures 1A and 1C). However, 21 days after primary immunization, the spleens of mice with enforced NF-κB activation alone or together with *BLIMP1* loss were virtually devoid of GFP^{pos} GC B cells (Figures 1B and 1C). Although constitutive NF-κB activation did not affect *AICDA* transcript levels in GC B cells 10 days after immunization, the few remaining GC B cells in these mice on day 21 post-immunization carried a significantly lower number of somatic mutations in their Ig heavy chain (IgH) V regions compared to controls (Figures 1E and 1F). Collectively, these results suggest that constitutive NF-κB activity promotes premature termination of the GC reaction through both BLIMP1-dependent and -independent mechanisms, thereby reducing the load of somatic mutations in the GC progeny.

With respect to cell proliferation, *BLIMP1* deletion in GC B cells, with or without concomitant activation of NF-κB, resulted in a small, but significant increase of the fraction of cells in the S and G2 phases of the cell cycle, compared to controls (Figure 2A). This could be due to the loss of BLIMP1 (Figure 1D), which is thought to repress genes promoting cell cycle progression, in the small fraction (0.5%–4%) of BLIMP1^{pos} GC B cells (Angelin-Duclos et al., 2000; Lin et al., 1997; Martins and Calame, 2008). In accord with the notion of an antiproliferative effect of BLIMP1, its acute ablation also promoted the proliferation of B cells in an in vitro cell culture system that mimics T cell-dependent B cell activation (Figures 2B–2D). In this in vitro cell culture system, the efficiency of Cre-mediated recombination was identical in B cells from mice of the various genotypes and virtually complete by day 3 of culture, as measured by the expression of the reporter genes (Figure 2B).

Interestingly, enforced *IKK2ca* expression in the in vitro system not only inhibited apoptosis of the ABCs (Figure 2E) but also enhanced their proliferation and cooperated with *BLIMP1* loss in accumulating increased numbers of cells over the 5-day culture period (Figures 2C and 2F). These results contrast with both the absence of an effect of enforced *IKK2ca* expression on the cell cycle distribution of GC B cells in vivo (Figure 2A) and the *IKK2ca*-mediated premature termination of the GC reaction (Figure 1). We considered the possibility that constitutive NF-κB signaling in GC B cells might interfere with *BCL6* expression (Saito et al., 2007) but could not detect such an effect when we analyzed *BCL6* mRNA expression by quantitative PCR (data not shown).

Ablation of *BLIMP1* Precludes Plasma Cell Formation

As expected from the literature (Martins and Calame, 2008), ablation of *BLIMP1* in B cells through Cγ1-cre severely impeded plasma cell formation in both *Cγ1-cre;Blimp1*^{FF}*eYFP*^{stopFL} and *Cγ1-cre;Blimp1*^{FF}*IKK2ca*^{stopFL} mice, 10 days after primary and secondary immunization (Figures 3A and 3B; see Figures S1A and S1B, available online), accompanied by a strong reduction of total as well as SRBC-specific IgG1, but not IgM, antibodies in the sera of the animals (Figure 3C; Figure S1C; data not shown). Thus, in agreement with BLIMP1's essential role in terminal B cell differentiation, its inactivation in our experimental system blocks plasma cell differentiation, also when combined with constitutive NF-κB activation. In contrast, activation of NF-κB alone was compatible with plasma cell differentiation (Figures 3A and 3B; Figures S1A, and S1B), and antibody titers in the sera of *Cγ1-cre;IKK2ca*^{stopFL} mice 10 days after primary immunization were similar to those in control mice (Figure 3C; Figure S1C).

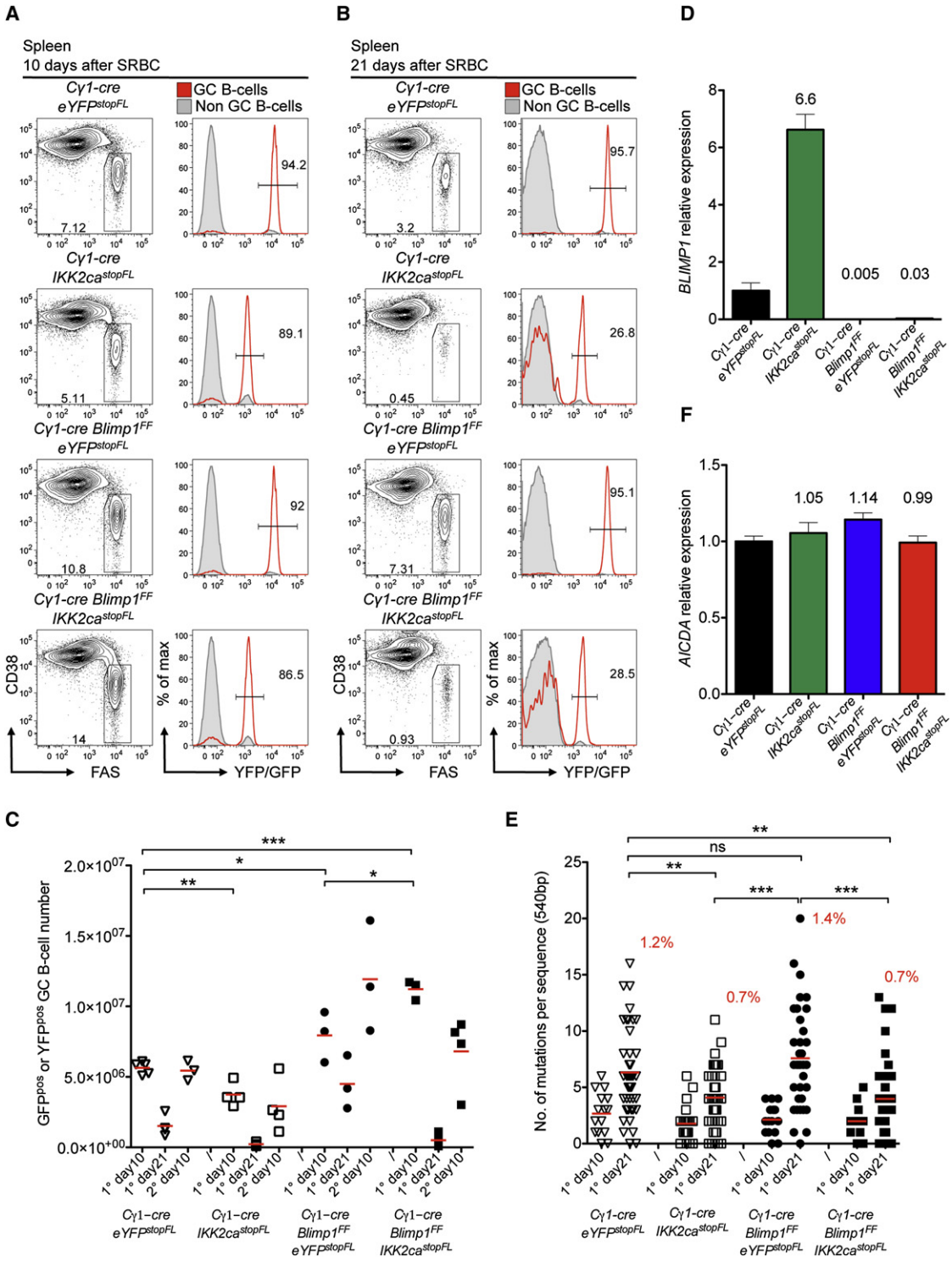

Figure 1. Impact of Constitutive NF-κB Activation and *BLIMP1* Deletion on the GC Reaction

(A) Left panel shows analysis by flow cytometry of the GC B cell population ($CD19^{pos}B220^{Pos}CD38^{Low}Fas^{High}$) in spleen 10 days after primary immunization with SRBCs of at least three mice per genotype. Right panel demonstrates reporter expression in GC B cells.

(B) Analysis of GC B cells as in (A) 21 days after primary immunization with SRBCs of at least three mice per genotype.

(C) Number of reporter-positive GC B cells in spleen at days 10 (1° day 10) and 21 (1° day 21) after primary immunization and of mice re-immunized 30 days after primary immunization and analyzed 10 days thereafter (2° day 10). Red bar represents mean of at least three mice per genotype.

(D) Relative *BLIMP1* transcript levels in reporter-positive GC B cells at day 10 after primary immunization. Values represent normalized levels to *HPRT*, relative to control ($C\gamma1\text{-}cre;eYFP^{stopFL}$). Data are represented as mean ± SEM of three mice per genotype. Numbers in graph represent mean value.

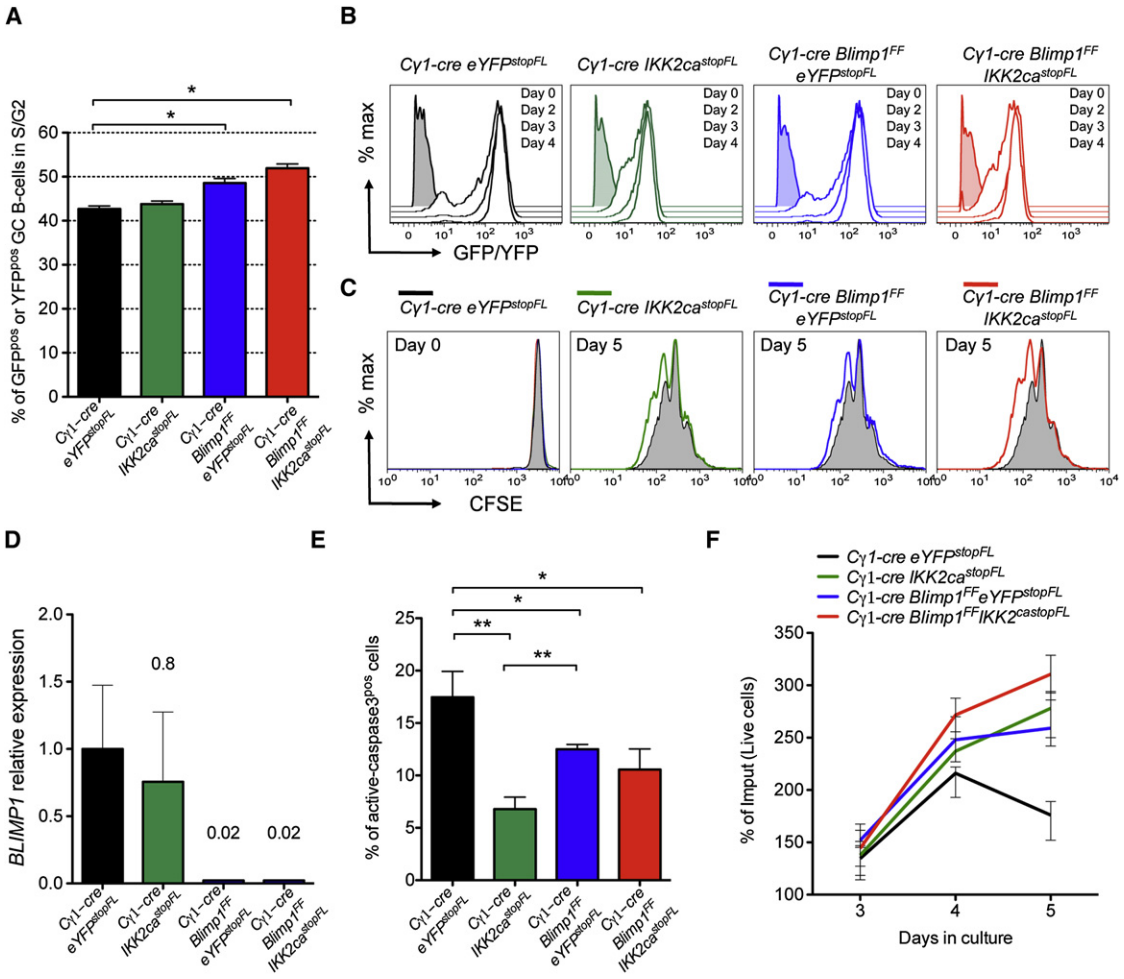

Figure 2. B Cell Proliferation and Survival upon *BLIMP1* Deletion and Constitutive NF-κB Activation

(A) DNA content of reporter-positive GC B cells at day 10 after primary immunization was determined using the Draq5 DNA-binding reagent and flow cytometry. Data are represented as mean ± SEM of four mice per genotype.

(B) Cre-mediated recombination efficiency measured by expression of reporter genes in purified B cells from compound mutant mice and control, cultured in vitro in the presence of αCD40 plus IL4. Data are representative of three independent experiments.

(C) CFSE dilution profile of in vitro cultured splenic B cells 5 days after stimulation with αCD40 plus IL4 from mice of the indicated genotypes. Data are representative of three independent experiments.

(D) Relative *BLIMP1* transcript levels in in vitro cultured splenic B cells 4 days after stimulation with αCD40 plus IL4 from mice of the indicated genotypes. Values represent normalized levels to *HPRT*, relative to control (*Cγ1-cre;eYFP*^{stopFL}). Data are represented as mean ± SEM of three independent experiments. Numbers in graph represent mean values.

(E) Frequency of apoptotic cells within in vitro-cultured splenic B cells 5 days after stimulation with αCD40 plus IL4 from mice of the indicated genotypes. Data are represented as mean ± SEM of three independent experiments.

(F) Percent (%) live cells relative to input in in vitro-cultured splenic B cells at days 3, 4, and 5 after stimulation with αCD40 plus IL4 from mice of the indicated genotypes. Percent (%) live cells relative to input is calculated based on the cell number of live cells at days 3, 4, and 5 relative to the cell number of live cells at day 0. Data are represented as mean ± SEM of three independent experiments.

Shortened Life Span of Mice upon B Cell-Specific BLIMP1 and IKK2ca Mutation

To assess the role of constitutive activation of the canonical NF-κB pathway and/or disruption of *BLIMP1* in lymphomagenesis, we generated cohorts of compound mutant mice and monitored them for tumor formation over a period of 550 days. Mice with enforced expression of *IKK2ca* alone showed a similar life span as control mice (Figure 4). In contrast, deletion of *BLIMP1*

(E) IgH somatic mutation in reporter-positive GC B cells at day 10 (eight or more sequences per mouse from at least two mice per genotype) and day 21 (ten or more sequences per mouse from at least three mice per genotype) after primary immunization with SRBCs. Red bar represents mean. Average mutation frequency at day 21 is given in red.

(F) Relative *AICDA* transcript levels in reporter-positive GC B cells at day 10 after primary immunization. Values represent normalized levels to *HPRT*, relative to control (*Cγ1-cre;eYFP*^{stopFL}). Data are represented as mean ± SEM of three mice per genotype. Numbers in graph represent mean value.

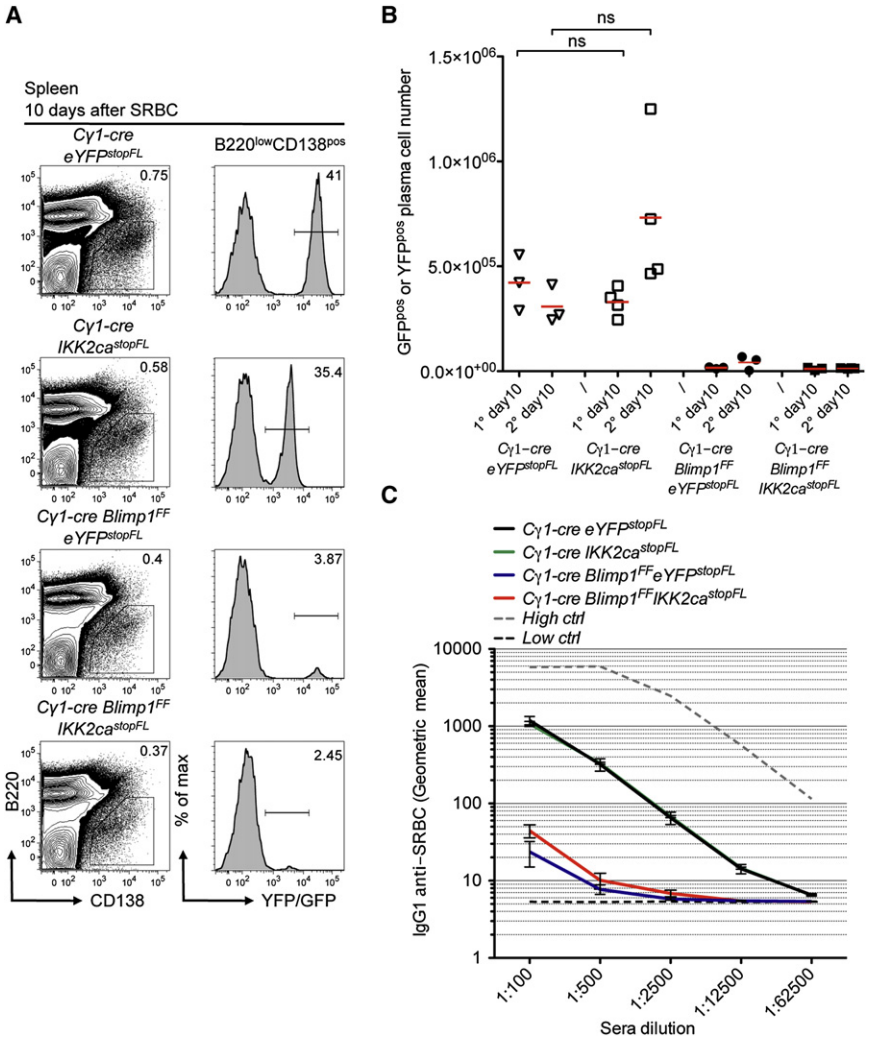

Figure 3. *BLIMP1* Inactivation Dominantly Abrogates Plasma Cell Formation

(A) Left panel shows flow-cytometric analysis of splenic plasma cells ($B220^{Low}CD138^{Pos}$) at day 10 after primary immunization of at least three mice per genotype. Right panel demonstrates frequency of reporter-positive plasma cells.

(B) Reporter-positive plasma cell numbers in spleen at day 10 after primary immunization and secondary immunization. Red bar represents mean of at least three mice per genotype.

(C) SRBC-specific IgG1 serum antibodies at day 10 after primary immunization. Data are represented as mean ± SEM of three mice per genotype. Low ctrl, unimmunized mice; High ctrl, serum from mice hyperimmunized with SRBCs. See also Figure S1.

in GC B cells led to shortened mouse survival, a phenotype further enhanced by the constitutive activation of the canonical NF-κB pathway (Figure 4).

Plasma Cell Hyperplasia in Mice with Constitutive Canonical NF-κB Activation

Macroscopic examination of *Cγ1-cre;IKK2ca*^{stopFL} mice, sacrificed between 550 and 600 days of age, revealed the presence of enlarged spleens in all cases (six of six), with a significant hyperplasia of both B and plasma cells in spleen and bone marrow (Figures 5A and 5B; Figures S2A and S2B). Accordingly, large numbers of cells expressing intracellular Ig and the plasma cell marker CD138 could be detected in splenic histological sections of these mice, whereas there was essentially no expression of the GC B cell marker PNA (Figure 5C; data not shown). Consistent with the increased numbers of plasma cells, the serum titers of both IgM and IgG1 were higher in *Cγ1-cre; IKK2ca*^{stopFL} mice than controls (Figure S2C). Electrophoretic analysis of sera from these mice revealed the presence of distinct band(s) in the γ-globulin region of the gel (M-spikes) in 70% of *Cγ1-cre;IKK2ca*^{stopFL} mice (seven of ten) compared to 20% (two of ten) of controls, indicative of clonal or oligoclonal plasma cell expansions (Figure 5D; data not shown). Thus, constitutive activation of the NF-κB canonical pathway promotes not only B cell hyperplasia, consistent with our previous results (Sasaki et al., 2006), but also plasma cell hyperplasia.

B Cell-Specific *BLIMP1* Inactivation Leads to B Cell Lymphomagenesis

Examination of terminally ill *Cγ1-cre; Blimp1*^{FF}*eYFP*^{stopFL} mice revealed splenomegaly in all cases (11/11), occasionally together with lymphadenopathy, and hepatomegaly in one case (Figure 6A; data not shown). Histological analysis of enlarged spleens and lymph nodes showed in six of seven mice examined the presence of large cells with a diffuse growth pattern, resembling human DLBCL (Figure 6B). These cells were immunohistochemically negative for CD138 and intracellular Ig but expressed the B cell marker CD19 and, thus, represented transformed B rather than plasma cells (Figure 6C; data not shown). The analysis of IgH gene rearrangements by Southern blot in spleen and lymph nodes revealed that the lymphoproliferations were of clonal origin in six of eight cases (Figure 6D). We succeeded in amplifying IgH rearrangements from three clonal tumors by PCR and found that two of them were highly somatically mutated, whereas the third one carried a single nucleotide exchange (Table S1). We then assessed whether these lymphomas resembled a particular DLBCL subtype. Expression of *MUM1/IRF4* as identified by immunohistochemical staining correlates with ABC-, whereas *BCL6* expression is primarily associated with GCB-DLBCL (Choi et al., 2009; Hans et al., 2004), although a fraction of ABC-DLBCLs is also positive for BCL6 (Alizadeh et al., 2000; Iqbal et al., 2007; Lenz and Staudt, 2010). Consistent with an ABC-DLBCL phenotype, five of six DLBCLs arising in *Cγ1-cre; Blimp1*^{FF}*eYFP*^{stopFL} mice were $IRF4^{pos}BCL6^{neg}$ by immunohistochemical staining, whereas the remaining case was

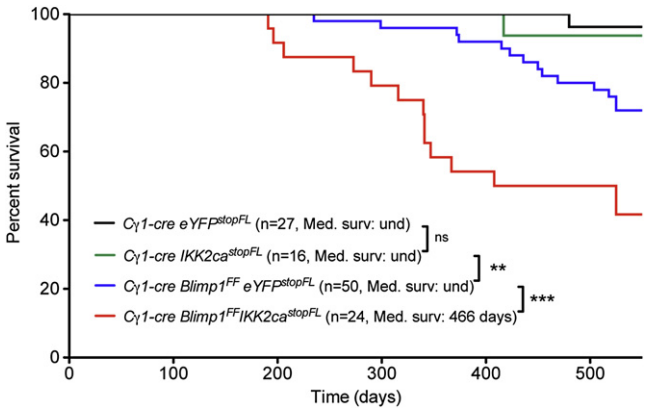

Figure 4. Survival of Mice Carrying the *Cγ1-cre* Transgene Together with *Blimp1*^{F}, *IKK2ca*^{stopFL}, or Both Alleles

Kaplan-Meier survival graph of mice of the indicated genotypes. Med. surv, median survival; und, undefined.

IRF4^{neg}BCL6^{pos} and in addition stained for the GC B cell marker PNA (Figure 6E; Figures S3A and S3B). Because *IRF4* is a target of the NF-κB pathway (Grumont and Gerondakis, 2000; Saito et al., 2007), and most human ABC-DLBCLs show NF-κB activation, we looked at whether this pathway was activated in lymphomas arising upon *BLIMP1* loss. Using the YFP reporter as a marker, we purified lymphoma cells from the IRF4^{neg}BCL6^{pos} (L1) and two IRF4^{pos}BCL6^{neg} (L2, L3) lymphomas, for which we had material available, and determined the transcript levels of known NF-κB target genes frequently expressed in human ABC-DLBCL (Alizadeh et al., 2000). Consistent with a GCB-DLBCL phenotype, the L1 lymphoma had low expression of NF-κB target genes and elevated transcript levels of GC B cell markers (Figure 6F). In contrast the L2 and L3 lymphomas showed elevated expression of some (*NFKBIA*, *PIM2*, *BCL2)* or all NF-κB target genes tested but low transcript levels of GC B cell markers (Figure 6F). We searched for mutations of the *A20*, *CARD11*, and *CD79a* and *b* genes in these cells, which have been associated with constitutive NF-κB activation in human ABC-DLBCL. However, no such mutations were detected by sequence analysis of amplified cDNAs. We also tested the expression levels of non-NF-κB target genes typically expressed in human ABC-DLBCL (Wright et al., 2003), including the transcription factor *FOXP1*, indicative of a poor clinical prognosis (Banham et al., 2005; Lenz and Staudt, 2010). Both L2 and L3 had elevated levels of *FOXP1* compared to GC B cells; however, only L3 showed expression of the majority of the other ABC-DLBCL associated genes tested (Figure 6F). Together, our results demonstrate that *BLIMP1* inactivation promotes lymphoma development in the mouse, in agreement with the recent results of others (Mandelbaum et al., 2010 [this issue of *Cancer Cell*]). In addition the lymphomas arising in these mice often show molecular features of human ABC-DLBCL.

Synergy between NF-κB Activity and *BLIMP1* Loss in B Cell Lymphomagenesis

Mice with combined *BLIMP1* deletion and activation of the NF-κB pathway had a significantly reduced life span compared to mice with *BLIMP1* inactivation alone (Figure 4). Similar to the latter, these mice succumbed to a B cell-derived lymphoproliferative disease affecting spleen and lymph nodes, showing in all five cases analyzed morphological features resembling human DLBCL (Figures 6A–6C; data not shown). Analysis of IgH rearrangements by Southern blot showed that these mice develop clonal lymphomas (Figure 6D). Sequence analysis of the clonal IgH rearrangements amplified by PCR revealed the presence of several somatic point mutations in one case and a single nucleotide exchange in another, whereas no mutations could be detected in two other cases. These latter tumors, like the one with a single mutation, expressed IgM on their surface (Table S1). Consistent with an ABC-DLBCL phenotype and constitutive NF-κB activation, five of five lymphomas analyzed were IRF4^{pos}BCL6^{neg} by immunohistochemical staining (Figure 6E; Figure S3A). Analysis of purified (GFP^{pos}) tumor cells from three of these lymphomas for which we had material available (L4, L5, L6) revealed low expression of GC B cell markers and elevated transcript levels for most of the ABC-DLBCL associated NF-κB target and nontarget genes tested, compared to GC B cells (Figure 6F). Collectively, these results reveal a strong cooperative effect between constitutive activation of the canonical NF-κB pathway and *BLIMP1* loss in the pathogenesis of lymphomas resembling human ABC-DLBCL.

DISCUSSION

Using conditional mutagenesis in GC B cells in the mouse, we show that *BLIMP1* disruption promotes the development of lymphomas often resembling human ABC-DLBCL. This is in full accord with the results of Mandelbaum et al. (2010). The low penetrance, long latency, and clonality of DLBCL in these mice suggested that additional oncogenic events are required for the pathogenesis of this disease. A major candidate for one such event is the NF-κB pathway because the majority of human ABC-DLBCLs display constitutive NF-κB activation, and most lymphomas arising upon conditional *BLIMP1* deletion in mice also show activation of this pathway. Indeed, we found that constitutive activation of the canonical NF-κB pathway strongly synergized with loss of *BLIMP1* in lymphomagenesis. Thus, our work suggests that both NF-κB signaling and the loss of *BLIMP1* play causal roles in the pathogenesis of human ABC-DLBCL.

Similar to ABC-DLBCL, genetic alterations leading to constitutive NF-κB activation have been described in multiple myeloma, suggesting a role for this pathway in the pathogenesis of this disease (Annunziata et al., 2007; Keats et al., 2007; Staudt, 2010). Supporting this concept, we found that constitutive activation of NF-κB through the Cγ1-cre transgene promotes plasma cell hyperplasia. If ABC-DLBCLs indeed derive from an ABC at an early stage of plasma cell differentiation (Lenz and Staudt, 2010), these results in turn indicate that the pathogenesis of this disease necessarily requires interference with terminal B cell differentiation, as exemplified by *BLIMP1* inactivation.

Besides abrogating B cell terminal differentiation, the loss of *BLIMP1* may promote cellular proliferation through derepression of BLIMP1 target genes controlling cell cycle progression (Lin et al., 1997; Martins and Calame, 2008). Constitutive activation of the canonical NF-κB pathway, on the other hand, releases B cells from their dependence of extracellular survival signals,

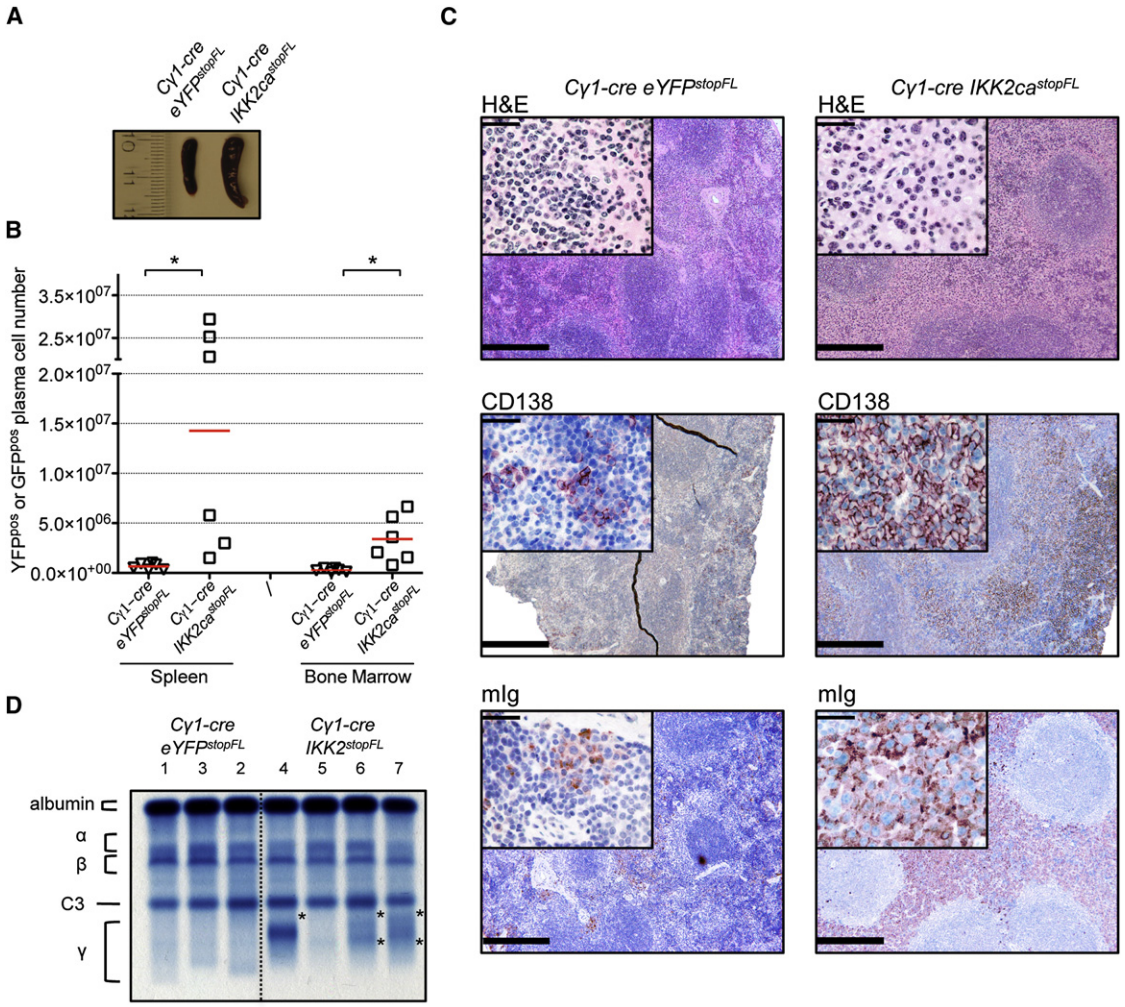

Figure 5. Constitutive Canonical NF-κB Signaling Promotes Plasma Cell Hyperplasia

(A) Representative picture of spleens from ≥550-day-old mice of the indicated genotypes. Six mice per genotype were analyzed.

(B) Absolute number of reporter-positive plasma cells ($CD19^{neg}CD138^{pos}$) in spleen and bone marrow of ≥550-day-old mice of the indicated genotypes. Red bar represents mean of at least six mice per genotype.

(C) Representative immunohistochemical staining of spleens from ≥550-day-old mice of the indicated genotypes. Upper panel shows H&E, middle panel CD138, and lower panel intracellular Ig. Six mice were analyzed per genotype. Scale bar, 1000 μm; inset, 100 μm.

(D) Representative serum protein electrophoresis of sera from ≥550-day-old mice of the indicated genotypes. The position of albumin and of other components of the serum is indicated. * indicates M-spike/s. At least ten mice per genotype were analyzed. See also Figure S2.

such as BAFF, and although by itself not promoting cell division, enhances the proliferative response of mitogen-stimulated B cells (Sasaki et al., 2006). Thus, the cooperative effect of *BLIMP1* disruption and constitutive NF-κB signaling in the pathogenesis of human ABC-DLBCL likely results from blocking the differentiation of an ABC that displays deregulated proliferative and survival properties.

The increased and abnormally prolonged GC reaction in *Cγ1-cre;Blimp1^{FF}eYFP^{stopFL}* mice in conjunction with the presence of somatically mutated Ig gene rearrangements in the lymphomas arising upon *BLIMP1* deletion suggests that the latter likely originate predominantly from either a late or a post-GC B cell. The situation is less clear in the case of *BLIMP1* ablation in combination with activation of the NF-κB pathway, where we did not detect somatic mutations in the majority of the tumors. It is possible that this reflects an inherent feature of our experimental approach, in that NF-κB activation early on in the GC reaction leads to its premature termination (Bolduc et al., 2010; Kishi et al., 2010; and the present work). It may become significant in this situation that the *Cγ1-cre* transgene induces Cre-mediated recombination also in a small fraction of IgM-expressing non-GC B cells, whose absolute numbers easily compare to those of GC B cells (Casola et al., 2006). Such cells likely include antigen ABCs that have not yet entered the GC reaction (Casola et al., 2006; Garside et al., 1998; Toellner et al., 1996) and to whose proliferative expansion and ultimate transformation Cre-mediated NF-κB activation and loss of *BLIMP1* would equally contribute, as in the case of B cells activated in the course of the GC reaction. Indeed, the lymphomas arising in the compound mutants and carrying unmutated Ig

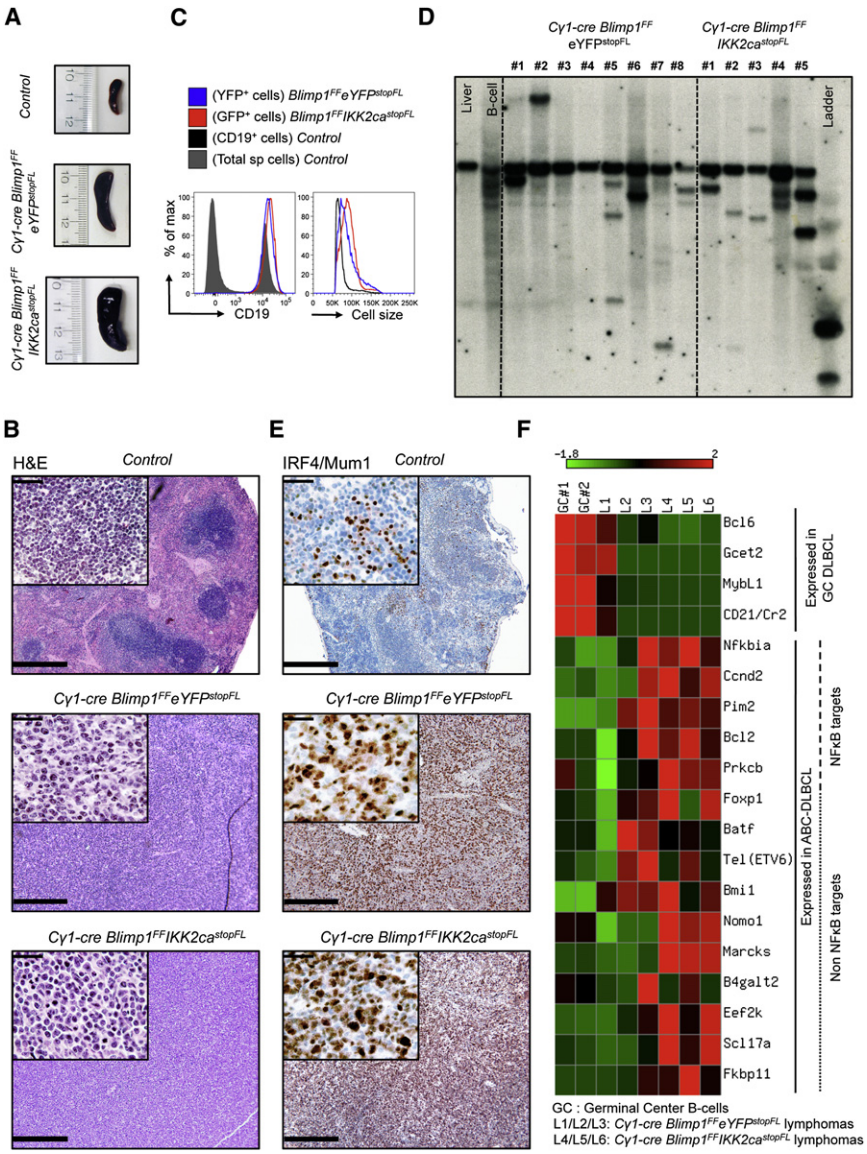

Figure 6. Mice with *BLIMP1* Deletion Alone and in Combination with Constitutive Canonical NF-κB Signaling Develop Lymphoma with an ABC Phenotype

(A) Representative pictures of spleens of compound mutant and control mice.

(B) Representative H&E staining of spleens of compound mutant (with six *Cγ1-cre;Blimp1^{FF}eYFP^{stopFL}* and five *Cγ1-cre;Blimp1^{FF}IKK2ca^{stopFL}* mice analyzed) and control mice. Scale bar, 1000 μm; inset, 100 μm.

(C) Representative analysis of cell size and CD19 expression of reporter-positive tumor cells from six *Cγ1-cre;Blimp1^{FF}eYFP^{stopFL}* and five *Cγ1-cre;Blimp1^{FF}IKK2ca^{stopFL}* mice and control mice.

(D) Southern blot analysis for tumor clonality using a J_H4 probe. Clonal tumors usually exhibit two bands corresponding to VDJ and DJ rearrangements.

(E) Representative immunohistochemical staining for MUM1/IRF4 of spleens of compound mutant (with five *Cγ1-cre;Blimp1^{FF}eYFP^{stopFL}* and five *Cγ1-cre;Blimp1^{FF}IKK2ca^{stopFL}* mice analyzed) and control mice. Scale bar, 1000 μm; inset, 100 μm.

(F) Heat map showing the relative transcript levels of candidate genes in lymphoma samples compared to GC B cells. For heat map generation the *HPRT*-normalized value of each candidate gene was normalized to have mean zero, variance one. See also Figure S3 and Table S1.

gene rearrangements expressed IgM on the cell surface. In this scenario the present mouse model reproduces the pathogenesis of a B cell lymphoma originating from the transformation of an ABC and, thus, of human ABC-DLBCL. However, in the latter case the activated COO usually represents a B cell in which the SHM mechanism is or has been operating because of its increased risk to accumulate unwanted mutational events (Lenz and Staudt, 2010). This feature applies less stringently in our system of conditional mutagenesis.

The lymphomas arising upon disruption of *BLIMP1* alone and in combination with constitutive NF-κB activation in compound mutant mice are of clonal origin, suggesting that additional oncogenic event(s) occurred that led to the outgrowth of a particular B cell clone. Because of the similarity of these lymphomas with human ABC-DLBCL, the identification of these additional genetic lesions might lead to the discovery of critical players in ABC-DLBCL pathogenesis and open the way to new therapeutic strategies.

EXPERIMENTAL PROCEDURES

Mice, Immunization, and Tumor Cohorts

Cγ1-cre, *IKK2ca^{stopFL}*, *Blimp1^{FF}*, and *eYFP^{stopFL}* alleles have been described (Casola et al., 2006; Ohinata et al., 2005; Sasaki et al., 2006; Srinivas et al., 2001). Eight- to 10-week-old mice were immunized i.v. with 1 × 10^9 SRBCs (Cedarlane) in PBS. Mouse cohorts were monitored twice a week for tumor development under monthly antigenic stimulation by SRBC immunization and euthanized if signs of tumor development occurred. All animal care and procedures followed National Institutes of Health guidelines and were approved by the Institutional Animal Care and Use Committee (IACUC 03341) of Harvard University and the Immune Disease Institute.

Flow Cytometry

Lymphoid single-cell suspensions were stained with the following monoclonal antibodies from BD: αCD19(ID3), αB220(RA3-6B2), αCD95(Jo2), αCD138 (281-2), and αCD38(90). Samples were acquired on a FACSCanto II (BD) and analyzed using FlowJo software (Tree Star, Inc.).

ELISA and SRBC-Specific Antibody Detection

ELISA was performed as described (Casola et al., 2006). For detection of SRBC-specific IgG1, 2 × 10^6 SRBCs were incubated with sera for 20 min at 4°C, washed twice with 1 × PBS, and then incubated with αmouseIgG1 (A85-1; BD) antibody for 20 min at 4°C. After one wash with 1 × PBS, the geometric mean of the fluorescence intensity was determined through the acquisition of SRBC samples by flow cytometry.

Serum Protein Electrophoresis

Serum was diluted 1:2 in barbital buffer and analyzed on a Hydragel K20 system according to manufacturer's instruction (Sebia).

Real-Time PCR and Heat Map Generation

Total RNA was extracted using TRIzol reagent, and cDNA was synthesized using the ThermoScript RT-PCR System (Invitrogen). For qRT-PCR we used Power SYBR Green, followed by analysis with the StepOnePlus System (Applied Biosystems). Samples were assayed in duplicate, and messenger abundance was normalized to that of *HPRT*. To detect *BLIMP1* transcripts we used a primer set pairing in the exon 4-5 junction. Because in the *Blimp1*^{F} allele exon 5 is *loxp* flanked and will be deleted upon Cre-mediated recombination (Ohinata et al., 2005), we used this primer set to confirm *BLIMP1* deletion. Heat map was generated using the Matrix2png software (Pavlidis and Noble, 2003).

Analysis of Tumor Clonality

This was done by Southern blotting of EcoRI-digested genomic DNA from tumors using a J_H probe spanning the J_H4 exon and part of the downstream intronic sequence.

Histology

Tissues were fixed with 10% formalin (Sigma), and paraffin-embedded sections were stained with hematoxylin and eosin (H&E; Sigma), αIRF4 (MUM1; Santa Cruz), αBCL6 (sc-C19; Santa Cruz), PNA (Vector), αCD138 (281-2; BD), and αmIg (Vector).

GC B Cell DNA Content Analysis

Cells were stained for surface markers and fixed with 2% formaldehyde for 15 min at RT and then incubated with the DNA-binding agent Draq5 (Biostatus) at a final concentration of 12.5 μM for 30 min at RT. Samples were acquired and analyzed as above. Cell cycle analysis was performed using the Watson-Pragmatic computational model in FlowJo software.

IgH Somatic Mutation Analysis

Genomic DNA was prepared from tumor tissues or sorted B cells. IgH-V gene rearrangements were PCR amplified using the Expand High Fidelity PCR System (Roche) and forward primers V_HA and V_HE (Ehlich et al., 1994), and a reverse primer in the J_H4 intron (5′-CTCCACCAGACCTCTCTAGACAGC-3′). Fragments were cloned, sequenced, and blasted against the NCBI database (http://www.ncbi.nlm.nih.gov/igblast/) to determine $V_HD_HJ_H$ usage. The cloned intronic sequences were then aligned to their germline counterparts. In determining somatic mutations we excluded polymorphisms associated with the *Cγ1-cre* allele.

In Vitro Cell Culture, CFSE Labeling, and Detection of Apoptotic Cells

Splenic B cells were purified by CD43 depletion (Miltenyi). Cells were cultured in the presence of 1 μg/ml αCD40 (HM40-3; eBioscience) and 25 ng/ml IL-4 (R&D Systems). To monitor cellular division, B cells were labeled in 1 ml 2.5 μM CFSE (Invitrogen) in 1 × PBS per 10^7 cells at 37°C for 10 min. Before acquisition of CFSE-labeled cells by flow cytometry, inactivation of GFP or YFP fluorescence was achieved by fixing cells using a Fix/Perm reagent (eBioscience). Cells undergoing apoptosis were detected using the Active Caspase-3 Apoptosis Kit (BD), according to manufacturer's instructions.

Statistical Analysis

Data were analyzed using unpaired two-tailed Student's t test; a p value ≤ 0.05 was considered significant. A single asterisk (*) in the graphs of figures represents a p value ≤ 0.05, double asterisks (**) a p value ≤ 0.01, and triple asterisks (***) a p value ≤ 0.001, and "ns" stands for not statistically significant, i.e., a p value >0.05. Survival curves were compared using the log rank test. Data in text and figures are represented as mean ± standard error of the mean (SEM).

SUPPLEMENTAL INFORMATION

Supplemental Information includes Supplemental Experimental Procedures, three figures, and one table and can be found with this article online at doi:10.1016/j.ccr.2010.11.024.

ACKNOWLEDGMENTS

We thank D. Ghitza, A. Pellerin, J. Grundy, and J. Xia for technical assistance, M. Ottaviano for administrative assistance, K.R. laboratory members, M. Janz and S.A. Godinho for critical comments and suggestions, S. Koralov for help with sequence analysis, and S. Peng for *HPRT* qRT-PCR primers. K.R. is supported by the National Cancer Institute through P01CA092625 and an LLS SCOR grant, and D.P.C. and B.Z. by postdoctoral fellowships of the Leukemia & Lymphoma Society. The authors declare no conflict of interest.

Received: July 26, 2010
Revised: October 26, 2010
Accepted: November 15, 2010
Published: December 13, 2010

REFERENCES

Alizadeh, A.A., Eisen, M.B., Davis, R.E., Ma, C., Lossos, I.S., Rosenwald, A., Boldrick, J.C., Sabet, H., Tran, T., Yu, X., et al. (2000). Distinct types of diffuse large B-cell lymphoma identified by gene expression profiling. Nature *403*, 503–511.

Angelin-Duclos, C., Cattoretti, G., Lin, K.I., and Calame, K. (2000). Commitment of B lymphocytes to a plasma cell fate is associated with Blimp-1 expression in vivo. J. Immunol. *165*, 5462–5471.

Annunziata, C.M., Davis, R.E., Demchenko, Y., Bellamy, W., Gabrea, A., Zhan, F., Lenz, G., Hanamura, I., Wright, G., Xiao, W., et al. (2007). Frequent engagement of the classical and alternative NF-kappaB pathways by diverse genetic abnormalities in multiple myeloma. Cancer Cell *12*, 115–130.

Banham, A.H., Connors, J.M., Brown, P.J., Cordell, J.L., Ott, G., Sreenivasan, G., Farinha, P., Horsman, D.E., and Gascoyne, R.D. (2005). Expression of the FOXP1 transcription factor is strongly associated with inferior survival in patients with diffuse large B-cell lymphoma. Clin. Cancer Res. *11*, 1065–1072.

Bolduc, A., Long, E., Stapler, D., Cascalho, M., Tsubata, T., Koni, P.A., and Shimoda, M. (2010). Constitutive CD40L expression on B cells prematurely terminates germinal center response and leads to augmented plasma cell production in T cell areas. J. Immunol. *185*, 220–230.

Casola, S., Cattoretti, G., Uyttersprot, N., Koralov, S.B., Seagal, J., Hao, Z., Waisman, A., Egert, A., Ghitza, D., and Rajewsky, K. (2006). Tracking germinal center B cells expressing germ-line immunoglobulin gamma1 transcripts by conditional gene targeting. Proc. Natl. Acad. Sci. USA *103*, 7396–7401.

Choi, W.W., Weisenburger, D.D., Greiner, T.C., Piris, M.A., Banham, A.H., Delabie, J., Braziel, R.M., Geng, H., Iqbal, J., Lenz, G., et al. (2009). A new immunostain algorithm classifies diffuse large B-cell lymphoma into molecular subtypes with high accuracy. Clin. Cancer Res. *15*, 5494–5502.

Compagno, M., Lim, W.K., Grunn, A., Nandula, S.V., Brahmachary, M., Shen, Q., Bertoni, F., Ponzoni, M., Scandurra, M., Califano, A., et al. (2009). Mutations of multiple genes cause deregulation of NF-kappaB in diffuse large B-cell lymphoma. Nature *459*, 717–721.

Davis, R.E., Brown, K.D., Siebenlist, U., and Staudt, L.M. (2001). Constitutive nuclear factor kappaB activity is required for survival of activated B cell-like diffuse large B cell lymphoma cells. J. Exp. Med. *194*, 1861–1874.

Davis, R.E., Ngo, V.N., Lenz, G., Tolar, P., Young, R.M., Romesser, P.B., Kohlhammer, H., Lamy, L., Zhao, H., Yang, Y., et al. (2010). Chronic active B-cell-receptor signalling in diffuse large B-cell lymphoma. Nature *463*, 88–92.

Ehlich, A., Martin, V., Muller, W., and Rajewsky, K. (1994). Analysis of the B-cell progenitor compartment at the level of single cells. Curr. Biol. *4*, 573–583.

Garside, P., Ingulli, E., Merica, R.R., Johnson, J.G., Noelle, R.J., and Jenkins, M.K. (1998). Visualization of specific B and T lymphocyte interactions in the lymph node. Science *281*, 96–99.

Grumont, R.J., and Gerondakis, S. (2000). Rel induces interferon regulatory factor 4 (IRF-4) expression in lymphocytes: modulation of interferon-regulated gene expression by rel/nuclear factor kappaB. J. Exp. Med. *191*, 1281–1292.

Hans, C.P., Weisenburger, D.D., Greiner, T.C., Gascoyne, R.D., Delabie, J., Ott, G., Muller-Hermelink, H.K., Campo, E., Braziel, R.M., Jaffe, E.S., et al. (2004). Confirmation of the molecular classification of diffuse large B-cell

lymphoma by immunohistochemistry using a tissue microarray. Blood *103*, 275–282.

Iqbal, J., Greiner, T.C., Patel, K., Dave, B.J., Smith, L., Ji, J., Wright, G., Sanger, W.G., Pickering, D.L., Jain, S., et al. (2007). Distinctive patterns of BCL6 molecular alterations and their functional consequences in different subgroups of diffuse large B-cell lymphoma. Leukemia *21*, 2332–2343.

Kato, M., Sanada, M., Kato, I., Sato, Y., Takita, J., Takeuchi, K., Niwa, A., Chen, Y., Nakazaki, K., Nomoto, J., et al. (2009). Frequent inactivation of A20 in B-cell lymphomas. Nature *459*, 712–716.

Keats, J.J., Fonseca, R., Chesi, M., Schop, R., Baker, A., Chng, W.J., Van Wier, S., Tiedemann, R., Shi, C.X., Sebag, M., et al. (2007). Promiscuous mutations activate the noncanonical NF-kappaB pathway in multiple myeloma. Cancer Cell *12*, 131–144.

Kishi, Y., Aiba, Y., Higuchi, T., Furukawa, K., Tokuhisa, T., Takemori, T., and Tsubata, T. (2010). Augmented antibody response with premature germinal center regression in CD40L transgenic mice. J. Immunol. *185*, 211–219.

Lenz, G., and Staudt, L.M. (2010). Aggressive lymphomas. N. Engl. J. Med. *362*, 1417–1429.

Lenz, G., Davis, R.E., Ngo, V.N., Lam, L., George, T.C., Wright, G.W., Dave, S.S., Zhao, H., Xu, W., Rosenwald, A., et al. (2008a). Oncogenic CARD11 mutations in human diffuse large B cell lymphoma. Science *319*, 1676–1679.

Lenz, G., Wright, G.W., Emre, N.C., Kohlhammer, H., Dave, S.S., Davis, R.E., Carty, S., Lam, L.T., Shaffer, A.L., Xiao, W., et al. (2008b). Molecular subtypes of diffuse large B-cell lymphoma arise by distinct genetic pathways. Proc. Natl. Acad. Sci. USA *105*, 13520–13525.

Lin, Y., Wong, K., and Calame, K. (1997). Repression of c-myc transcription by Blimp-1, an inducer of terminal B cell differentiation. Science *276*, 596–599.

Lossos, I.S., Alizadeh, A.A., Eisen, M.B., Chan, W.C., Brown, P.O., Botstein, D., Staudt, L.M., and Levy, R. (2000). Ongoing immunoglobulin somatic mutation in germinal center B cell-like but not in activated B cell-like diffuse large cell lymphomas. Proc. Natl. Acad. Sci. USA *97*, 10209–10213.

Mandelbaum, J., Bhagat, G., Tang, F., Mo, T., Brahmachary, M., Shen, Q., Chadburn, A., Rajewsky, K., Tarakhovsky, A., Pasqualucci, L., and Dalla-Favera, R. (2010). BLIMP1/PRDM1 is a tumor suppressor gene frequently disrupted in activated B-cell like diffuse large B cell lymphoma. Cancer Cell *18*, this issue, 568–579.

Martins, G., and Calame, K. (2008). Regulation and functions of Blimp-1 in T and B lymphocytes. Annu. Rev. Immunol. *26*, 133–169.

Monti, S., Savage, K.J., Kutok, J.L., Feuerhake, F., Kurtin, P., Mihm, M., Wu, B., Pasqualucci, L., Neuberg, D., Aguiar, R.C., et al. (2005). Molecular profiling of diffuse large B-cell lymphoma identifies robust subtypes including one characterized by host inflammatory response. Blood *105*, 1851–1861.

Ohinata, Y., Payer, B., O'Carroll, D., Ancelin, K., Ono, Y., Sano, M., Barton, S.C., Obukhanych, T., Nussenzweig, M., Tarakhovsky, A., et al. (2005). Blimp1 is a critical determinant of the germ cell lineage in mice. Nature *436*, 207–213.

Pasqualucci, L., Compagno, M., Houldsworth, J., Monti, S., Grunn, A., Nandula, S.V., Aster, J.C., Murty, V.V., Shipp, M.A., and Dalla-Favera, R. (2006). Inactivation of the PRDM1/BLIMP1 gene in diffuse large B cell lymphoma. J. Exp. Med. *203*, 311–317.

Pavlidis, P., and Noble, W.S. (2003). Matrix2png: a utility for visualizing matrix data. Bioinformatics *19*, 295–296.

Saito, M., Gao, J., Basso, K., Kitagawa, Y., Smith, P.M., Bhagat, G., Pernis, A., Pasqualucci, L., and Dalla-Favera, R. (2007). A signaling pathway mediating downregulation of BCL6 in germinal center B cells is blocked by BCL6 gene alterations in B cell lymphoma. Cancer Cell *12*, 280–292.

Sasaki, Y., Derudder, E., Hobeika, E., Pelanda, R., Reth, M., Rajewsky, K., and Schmidt-Supprian, M. (2006). Canonical NF-kappaB activity, dispensable for B cell development, replaces BAFF-receptor signals and promotes B cell proliferation upon activation. Immunity *24*, 729–739.

Srinivas, S., Watanabe, T., Lin, C.S., William, C.M., Tanabe, Y., Jessell, T.M., and Costantini, F. (2001). Cre reporter strains produced by targeted insertion of EYFP and ECFP into the ROSA26 locus. BMC Dev. Biol. *1*, 4.

Staudt, L.M. (2010). Oncogenic activation of NF-kappaB. Cold Spring Harb. Perspect. Biol. *2*, a000109.

Tam, W., Gomez, M., Chadburn, A., Lee, J.W., Chan, W.C., and Knowles, D.M. (2006). Mutational analysis of PRDM1 indicates a tumor-suppressor role in diffuse large B-cell lymphomas. Blood *107*, 4090–4100.

Toellner, K.M., Gulbranson-Judge, A., Taylor, D.R., Sze, D.M., and MacLennan, I.C. (1996). Immunoglobulin switch transcript production in vivo related to the site and time of antigen-specific B cell activation. J. Exp. Med. *183*, 2303–2312.

WHO. (2008). WHO Classification of Tumours of Haematopoietic and Lymphoid Tissues, Fourth Edition (Geneva: WHO Press).

Wright, G., Tan, B., Rosenwald, A., Hurt, E.H., Wiestner, A., and Staudt, L.M. (2003). A gene expression-based method to diagnose clinically distinct subgroups of diffuse large B cell lymphoma. Proc. Natl. Acad. Sci. USA *100*, 9991–9996.